

Original article

## Effect of different freeze drying cycle in *Semimembranous* and *Gluteus Medius* bovine muscles: changes on microstructure, colour, texture and physicochemical parameters

Valeria Messina,<sup>1,2\*</sup> Facundo Pieniazek<sup>1</sup> & Ana Sancho<sup>3</sup>

1 CINSO – UNIDEF (Strategic I & D for Defense)-MINDEF-CITEDEF-CONICET, Juan Bautista de la Salle 4970, (B1603ALO), Villa Martelli, Buenos Aires, Argentina

2 The National Council for Scientific and Technical Research (CONICET), Rivadavia 1917, C1033AAJ, Buenos Aires, Argentina

3 Food Technology Institute-INTA, (B1708WAB), Buenos Aires, Argentina

(Received 17 December 2015; Accepted in revised form 24 January 2016)

**Summary** The aim of the present research was to evaluate effects of freeze drying cycle in *Semimembranous* and *Gluteus Medius* bovine muscles (sp: Aberdeen Angus) for instant meal. Samples were analysed by Scanning electron microscopy; texture and colour parameters were analysed by image analysis and physicochemical properties by instrumental assays. Micrographs revealed that a higher porous size structure and shrinkage of muscle fibre diameter were obtained at  $-40$  °C. In *Semimembranous* and *Gluteus Medius* bovine muscles, significant difference ( $P < 0.0001$ ) was obtained for texture, colour and physicochemical parameters. Results revealed that colour, texture and physicochemical parameters were less affected when freeze drying cycle was performed at  $-40$  °C. Freeze drying cycle at  $-50$  and  $-60$  °C showed increases in lightness ( $L^*$ ) and yellowness ( $b^*$ ); decrease in redness ( $a^*$ ) and in water absorbing capability).

**Keywords** Freeze drying, image analysis, muscle tissue, quality.

### Introduction

Today's food industry and retailers are trying to address the growing demand for convenience by considerable expansion of pre-prepared meal solutions, such as ready to eat meals. Due to the socio-economic evolutions and the busy and hectic lifestyle, ready meals have become a popular meal solution for many people around the world (Muhamad & Karim, 2014).

Among the drying methods that are used in food processing industries, freeze drying is considered one of the most advanced methods for drying high value products sensitive to heat, since it prevents undesirable shrinkage and produces materials with high porosity, unchanged nutrition quality, superior taste, aroma, flavour and colour retention, as well as better rehydration properties, superior to those dried with conventional techniques (Vasiliki *et al.*, 2011). Freeze drying is expensive, but one way to reduce costs is by reducing process such as freezing time, drying, etc.

As consumers increase consumption of ready to eat meals, more emphasis is necessary to be placed on

how to maintain quality and to develop new and faster technologies for quality control. Quality parameters are usually measured by conventional techniques, such as sensory and instrumental methods which are time consuming and destructive to the product. An interesting alternative for analysing the surface of food products and quantifying appearance characteristics is to use computerised image analysis techniques (Mendoza *et al.*, 2012; Saini *et al.*, 2014). Computer vision analysis is a method that objectively measure colour patterns in non-uniformly coloured surfaces, and also determine other physical features such as image texture, morphological elements and defects (Kono *et al.*, 2014). Moreover, with the advantage of superior speed, accuracy and recent advances in hardware and software, computer vision has attracted a significant amount of research aimed at replacing human inspection.

The aim of the present research was to evaluate effects on different freeze drying cycle in *Semimembranous* and *Gluteus Medius* bovine muscles (sp: Aberdeen Angus) for instant meal. Quality and physicochemical parameters were analysed applying instrumental and image analysis techniques.

\*Correspondent: E-mail: vmessina@citedef.gob.ar

## Material and methods

### Cooking process and sample preparation

Bovine muscles were provided by an abattoir centre of Argentina. *Semimembranosus* (SM) ( $n = 2$ ) and *Gluteus Medius* (GM) ( $n = 2$ ) *sp.*: Aberdeen Angus, were cooked and prepared as described by one of the authors (Messina *et al.*, 2014).

### Freeze drying cycle

Freeze drying process was carried out in a pilot plant freeze dryer supplied with four trays designed by an Industrial constructor (Rifacor, Argentina). Freeze drying cycle was set at three different freezing rates ( $-40$ ,  $-50$  and  $-60$  °C) during 24 h and dried (40 °C) during 24, 48 and 72 h under a chamber pressure of 0.346 Pa: samples were extracted as follows:  $-40$  °C/40 °C for 24 h;  $-40$  °C/40 °C for 48 h;  $-40$  °C/40 °C for 72 h;  $-50$  °C/40 °C for 24 h;  $-50$  °C/40 °C for 48 h;  $-50$  °C/40 °C for 72 h;  $-60$  °C/40 °C for 24 h;  $-60$  °C/40 °C for 48 h;  $-60$  °C/40 °C for 72 h), packaged, individually identified and stored in a dark place at room temperature until analysis.

### Scanning electron microscopy

Scanning electron microscopy was used for the observation of the microstructure of cooked freeze dried (CFD) and cooked freeze dried rehydrated (CFDR) samples of SM and GM. Samples were cross sectioned using a scalpel; the cut was always performed in the same direction. Samples were mounted on holders and coated with gold (Messina *et al.*, 2014). Microscopic evaluation was performed using a Scanning Electron Microscope (SEM 515; Philips, New York, NY, USA). Observations of the samples at magnification of 500 were obtained for image analysis (Model Genesis Version 5.21.). Brightness and contrast are the most important variables that must be controlled during the acquisition of images; therefore, the values of these parameters were kept constant for each magnification during the process of image acquisition.

### Colour and physicochemical parameters

Samples were illuminated using a lamp (model TL-D Deluxe, Natural Daylight, 18W/965; Philips) with a colour temperature of 6500 K (D65, standard light source) and a colour-rendering index (Ra) close to 90%. The four fluorescent tubes (60 cm long) were situated 35 cm above the sample and at an angle of 45° with the sample. Additionally, light diffusers covering each lamp and electronic ballast assured a uniform illumination system. A Color Digital Camera (CDC)

(Canon Eos Rebel, CANON, Tokyo, Japan) was located vertically over the sample at a distance of 12.5 cm. The angle between the camera lens and the lighting source axis was around 45°. Lamps and CDC were inside a wooden box with internal walls that were painted black to avoid the light and reflection from the room (Girolami *et al.* (2013).

Eighteen images from one side of each sample and eight regions of interest were taken on the matte black background using the following camera settings: manual mode with the lens aperture at  $f$  of 4.5 and speed 1/125, no zoom, no flash,  $3088 \times 2056$  pixels resolution of the CDC and storage in JPEG format. The algorithms for pre-processing of full images, image segmentation and colour quantification were processed by Adobe Photoshop cs6 (v13.0 Adobe Systems Incorporated, 2012).  $L$ ,  $a$  and  $b$  values were transformed to CIE  $L^*$ ,  $a^*$  and  $b^*$ . Values of  $L^*$ ,  $a^*$  and  $b^*$  were used to calculate Hue angle ( $h_{ab}^*$ ), where  $h_{ab}^* = 0^\circ$  for red hue and  $h_{ab}^* = 90^\circ$  for yellowish hue and chroma ( $C_{ab}^*$ ).

### Water activity and water absorbing capability

Water activity ( $a_w$ ) was performed using a Water Activity Meter (AquaLab 4TE, USA) and water absorbing capability (WAC) was performed as follows: 25 g of dried samples from each treatment were weighed and rehydrated in distilled water ( $98 \pm 1$  °C) until 60, 120, 240 and 360 s, then drained over a mesh for 30 s to eliminate the superficial water. The WAC was recorded as gram of water retained per gram of dried sample. All experiments were carried out in triplicate.

### Measurement of porosity

Porosity (P) was performed using a Stereopycnometer (Quantachrome multipycnometer Model MVP-1, USA) with an accuracy of  $0.001 \text{ cm}^3$ , utilising helium gas as described by Koc *et al.* (2008).

### Grey level co-occurrence matrix and image texture analysis

Eighteen SEM images samples and eight regions of interest of each acquired SEM images were selected. Textural property was computed from a set of Grey level co-occurrence (GLCM) probability distribution matrices for a given image. The GLCM shows the probability that a pixel of a particular grey level occurs at a specified direction and distance ( $d = 1$ ) from its neighbouring pixels. Grey level co-occurrence matrix is represented by  $P_{d,\theta}(i, j)$  where counts the neighbouring pair pixels with grey values  $i$  and  $j$  at the distance of  $d$  and the direction of  $\theta$ . Five image texture features [correlation (COR), energy (ASM),

homogeneity (HOM), entropy (ENT) and contrast (CON)] were calculated as follows (eqns 1–4), where  $\mu_x$ ,  $\mu_y$ ,  $\sigma_x$  and  $\sigma_y$  are the means and standard deviations of  $p_x$  and  $p_y$ .

$$\text{CON} = \sum_{i=0}^{n-1} \sum_{j=0}^{n-1} (i-j)^2 \text{Pd}, \theta(i,j) \quad (1)$$

$$\text{ENT} = - \sum_{i=0}^{n-1} \sum_{j=0}^{n-1} \text{Pd}, \theta(i,j)^2 \text{Log}P(i,j) \quad (2)$$

$$\text{HOM} = \sum_{i=0}^{n-1} \sum_{j=0}^{n-1} \frac{\text{Pd}, \theta(i,j)}{1 + |i-j|} \quad (3)$$

$$\text{ASM} = \sum_{i=0}^{N-1} \sum_{j=0}^{N-1} \text{Pd}, \theta(i,j)^2 \quad (4)$$

$$\text{COR} = \frac{\left[ \sum_{i=0}^{N-1} \sum_{j=0}^{N-1} (ij)P(ij) \right] - \mu_x \mu_y}{\sigma_x \sigma_y} \quad (5)$$

### Statistical analysis

Significant differences between means were determined by Tukey's test. A  $P$  value of 0.0001 was used to verify the significance of all tests. All statistical tests of this experiment were analysed using SPSS-Advanced Statistics 12 software (SPSS Inc., Chicago, IL, USA).

## Results and discussion

### Scanning electron microscopy

Figure 1 shows microstructure of CFDSM and CFDRSM and Fig. S1 CFDGM and CFDRGM. CFDSM and CFDGM structures appeared organised showing gaps among fibre bundles and between fibres. Myofibrils were dehydrated and separated and partially fragmented.

CFDSM and CFDGM samples frozen at  $-40^\circ\text{C}$  showed higher porous size structure with larger and irregular cavities when compared to  $-50$  and  $-60^\circ\text{C}$  due to higher diameter of ice crystals formed at  $-40^\circ\text{C}$ . On the other hand, CFDSM and CFDGM showed a homogenous structure at  $-40^\circ\text{C}$  at 72 h when it was compared to  $-40^\circ\text{C}$  at 24 and 48 h. Similar behaviour was observed for  $-50/-60^\circ\text{C}$  at 72 h. Kiani & Sun (2011) stated that crystallisation is a general term used to describe several different phenomena related to the formation of a crystalline lattice structure. This process consists of two main successive stages; nucleation and crystal growth. The interaction between these two steps determines the crystal characteristics, i.e. size, distribution and morphology of the crystals. Bevilacqua & Zaritzky (1980) reported that in freeze-dried *Semitendinosus muscle*, lower diameter of ice crystals ( $D$ ) were obtained when freezing temperature

decreased. The stated authors applied the following experimental equation to suggest relationship between the diameter of ice crystals ( $D$ ) and freezing temperature ( $t_c$ ), where  $a$  and  $b$  are regression constants.

$$D = a + b \ln t_c \quad (6)$$

Bald (1991) reported similar results as Bevilacqua & Zaritzky (1980) applying the following empirical model for growth of crystals, based on the relationship between the cooling rate and crystals size ( $D$ ), where  $D$  is mean crystal size,  $dT/dt$  is cooling rate at the freezing front and  $m$  and  $n$  are constants.

$$D = m(dT/dt)^{-n} \quad (7)$$

Micrographs of CFDGM and CFDSM also showed that CFDGM had higher porous size structure and shrinkage of fibre when compared to CFDSM. Changes in microstructure, probably due to that drying process induced faster denaturation of proteins and subsequently more reduction in dimension of myofibrils and collagen, resulting in shrinkage of muscle fibre diameter and sarcomere length (Kong *et al.*, 2008; Reyes *et al.*, 2011). CFDRSM and CFDRGM showed that due to porous size structure water easily reoccupied the empty spaces in all samples. In general, micrographs showed that a higher porous size structure due to ice sublimation during freeze drying process and shrinkage of muscle fibre diameter were observed for FDGM and FDSM at  $-40^\circ\text{C}$  when compared to  $-50$  and  $-60^\circ\text{C}$ .

### Colour parameters

Table 1 shows colour parameters of SM and GM muscles. Significant differences between colour values were obtained ( $P < 0.0001$ ). Results revealed that colour parameters are affected by freezing and drying time. Cycle performed at  $-40^\circ\text{C}$  seems to be less affected than  $-50$  and  $-60^\circ\text{C}$ . When different drying cycles were applied in FDSM and FDGM, lightness ( $L^*$ ) increased when freezing temperature decreased and drying time increased; Redness ( $a^*$ ) decreased when freeze drying decreased and drying time increased;  $b^*$ ,  $h_{ab}^*$  and  $C_{ab}^*$  increased when freezing temperature decreased and drying time increased. FDRGM and FDRSM showed that lightness ( $L^*$ ) decreased when freezing temperature decreased and drying time increased.  $b^*$ ,  $h_{ab}^*$  and  $C_{ab}^*$  increased when freezing temperature decreased and drying time increased.

An increase in  $L^*$  values is due to protein denaturation and/or shrinkage of the myofibrils, which tends to increase light scattering giving higher  $L^*$  values (Faustman *et al.*, 2010). On the other hand, freezing and thawing in bovine muscles produce an increase in



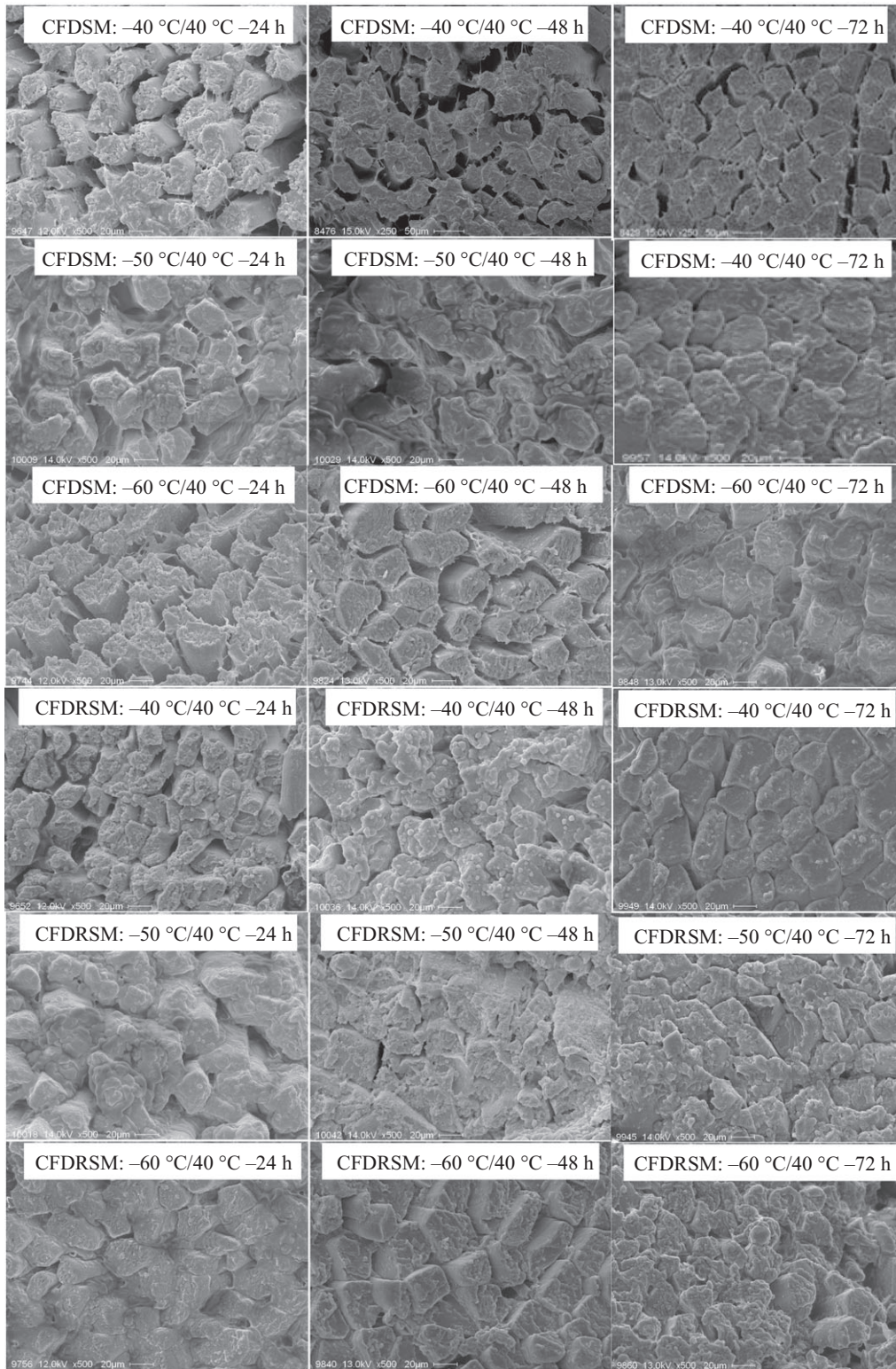


**Figure 1** Scanning micrographs performed at 500 time's magnification of cross sectional of cooked freeze dried (CFD) and cooked freeze dried rehydrated (CFDR) *Semimembranosus* muscle (SM) at different freeze drying cycles.

yellowness accompanied by a decrease in redness (Jeong *et al.*, 2011). Decrease in  $a^*$  values is due to oxidation of the central iron atom within the heme group, which is responsible for discoloration in meat, changing red (OxyMb) to brownish (MetMb).  $h_{ab}^*$  in meat is used to indicate the colour stability of fresh and processed meats. A decrease in  $h_{ab}^*$  indicates that colour becomes more stable and an increase in  $h_{ab}^*$  indicates that colour is less stable. These results suggest that increases in yellowness ( $b^*$ ) and in lightness ( $L^*$ ) are due to browning reactions between lipid oxidation products and the amine in the phospholipid head groups or the amine in proteins. Decrease in redness is caused by the formation of metmyoglobin leading to brownish colour in freeze-dried bovine muscle.

In general, results revealed that freezing  $-40$  °C and drying between 24 and 72 h, colour parameters are less affected when freezing temperature is decreased ( $-50$  and  $-60$  °C).

### Physicochemical parameters

#### Water activity

Significant differences between  $a_w$  values ( $P < 0.0001$ ) were obtained for CFDSM ( $a_w$   $_{-40} = 0.23$ ;  $a_w$   $_{-50/-60} = 0.18$ ); CFDGM ( $a_w$   $_{-40} = 0.21$ ; CFDGM ( $a_w$   $_{-50/-60} = 0.18$ ). Lower values of  $a_w$  generate secondary reactions that may affect attributes; it may produce higher oxymyoglobin production,  $b^*$  values increase (yellowness) due to accelerated oxidation taking place in the glassy state and a subsequent transformation of myoglobin (higher degree of oxidation) (Harnkarnsujarit *et al.*, 2014). Increases in  $a_w$ , accelerate lipid oxidation as well as degradation of polyphenols,  $\alpha$ -tocopherol among others (Baker *et al.*, 2002; Maltini *et al.*, 2003).

#### Porosity

Significant differences between porosity values ( $P < 0.0001$ ) were observed in both muscles. Mean values of CFDSM ( $-40$  °C ( $P_{24\text{ h}} = 60.90$ ;  $P_{48\text{ h}} = 60.83$ ;  $P_{72\text{ h}} = 60.72$ );  $-50$  °C ( $P_{24\text{ h}} = 69.80$ ;  $P_{48\text{ h}} = 69.76$ ;  $P_{72\text{ h}} = 69.76$ ) and  $-60$  °C ( $P_{24\text{ h}} = 72.65$ ;  $P_{48\text{ h}} = 72.62$ ;  $P_{72\text{ h}} = 72.61$ ) and CFDGM ( $-40$  °C ( $P_{24\text{ h}} = 52.60$ ;  $P_{48\text{ h}} = 52.59$ ;  $P_{72\text{ h}} = 52.59$ );  $-50$  °C ( $P_{24\text{ h}} = 60.0$ ;  $P_{48\text{ h}} = 59.9$ ;  $P_{72\text{ h}} = 59.8$ ) and  $-60$  °C ( $P_{24\text{ h}} = 69.9$ ;  $P_{48\text{ h}} = 69.8$ ;  $P_{72\text{ h}} = 69.7$ ) showed that higher amount of pores (porosity) were obtained at  $-60$  °C. Porosity in samples depends on different factors like cooking parameters, pressure and drying temperature. In freeze drying, high porosity (amounts of pores) helps to maintain the structure without the deformations that are inevitable in other drying methods (Leelayuthsoontorn & Thipayarat, 2006). The degree of porosity also has influence in texture and rehydration ability, when the size of the air cells in porous material

is bigger; it allows a fast rehydration due to that water easily enters and reoccupies the empty spaces (Oikonomopoulou *et al.*, 2011a,b). During subsequent freezing and freeze drying, the ice sublimation creates pores; the amount of pores (porosity) is related to the water uptake and is higher when the water uptake is increased. The porous structure is also influenced by the freezing process and a fast cooling with a high undercooling leads to smaller ice crystals and a larger inner surface. Due to the high porosity, the freeze-dried cell suspension has a high-specific surface area; this influences the sorption behaviour as well as the rehydration (Mounir, 2015). When porosity was related to SEM images, results showed that freeze drying at  $-40$  °C generated higher size pores, less amounts of pore and a more ordered structure appeared. Therefore, SEM micrographs with porosity confirm the based microstructure discussion presented above.

#### Water absorbing capability

WAC of CFDGM and CFDSM showed significant difference between values ( $P < 0.0001$ ). Results showed that higher WAC values were obtained at  $-40$  °C at 72 h in both muscles [FDRGM ( $R^2 = 0.987$  [ $-40$  °C];

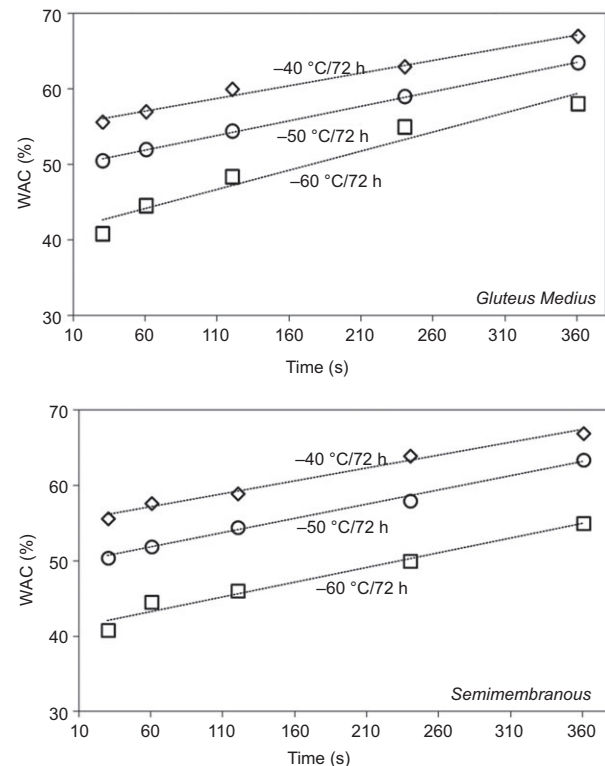


**Figure 2** Water absorbing capability of cooked freeze dried rehydrated *Gluteus medius* and *Semimembranosus* at different freeze drying cycle.

**Table 1** Colour parameters of *Semimembranosus* and *Gluteus medius* muscles (Sp: Aberdeen Angus)

Sample	Parameter	-40 °C			-50 °C			-60 °C			RSME	P value
		A	B	C	A	B	C	A	B	C		
FDGM	$L^*$	77.32 <sup>e</sup>	80.01 <sup>bc</sup>	80.61 <sup>bc</sup>	74.66 <sup>f</sup>	75.25 <sup>f</sup>	79.84 <sup>cd</sup>	81.55 <sup>b</sup>	81.78 <sup>b</sup>	83.74 <sup>a</sup>	0.3675	0.0001
FDGM	$a^*$	10.67 <sup>d</sup>	9.39 <sup>e</sup>	7.51 <sup>f</sup>	12.57 <sup>a</sup>	12.45 <sup>b</sup>	12.79 <sup>b</sup>	11.52 <sup>c</sup>	10.43 <sup>d</sup>	7.63 <sup>f</sup>	0.1576	0.0001
FDGM	$b^*$	23.80 <sup>f</sup>	24.60 <sup>e</sup>	25.54 <sup>d</sup>	27.43 <sup>c</sup>	28.51 <sup>b</sup>	28.44 <sup>b</sup>	27.46 <sup>c</sup>	28.17 <sup>b</sup>	29.52 <sup>a</sup>	0.1693	0.0001
FDGM	$h_{ab}^*$	65.89 <sup>f</sup>	69.14 <sup>c</sup>	73.65 <sup>b</sup>	65.41 <sup>f</sup>	65.82 <sup>f</sup>	66.44 <sup>e</sup>	67.28 <sup>d</sup>	69.72 <sup>c</sup>	75.55 <sup>a</sup>	0.2350	0.0001
FDGM	$C_{ab}^*$	26.08 <sup>d</sup>	26.60 <sup>d</sup>	26.62 <sup>d</sup>	30.17 <sup>b</sup>	31.10 <sup>a</sup>	31.78 <sup>a</sup>	29.78 <sup>c</sup>	30.04 <sup>b</sup>	30.49 <sup>b</sup>	0.2123	0.0001
FDRGM	$L^*$	72.62 <sup>d</sup>	79.46 <sup>b</sup>	79.52 <sup>b</sup>	70.11 <sup>e</sup>	76.54 <sup>c</sup>	76.88 <sup>c</sup>	76.85 <sup>c</sup>	81.38 <sup>a</sup>	81.32 <sup>a</sup>	0.2330	0.0001
FDRGM	$a^*$	7.12 <sup>d</sup>	7.22 <sup>d</sup>	7.48 <sup>d</sup>	10.51 <sup>a</sup>	9.52 <sup>b</sup>	9.29 <sup>b</sup>	8.44 <sup>c</sup>	8.51 <sup>c</sup>	8.53 <sup>c</sup>	0.2566	0.0001
FDRGM	$b^*$	21.84 <sup>c</sup>	21.99 <sup>c</sup>	23.19 <sup>d</sup>	23.62 <sup>ab</sup>	23.87 <sup>ab</sup>	24.34 <sup>a</sup>	20.73 <sup>d</sup>	23.21 <sup>b</sup>	23.66 <sup>ab</sup>	0.1456	0.0001
FDRGM	$h_{ab}^*$	71.57 <sup>d</sup>	71.86 <sup>d</sup>	83.94 <sup>a</sup>	66.05 <sup>h</sup>	68.29 <sup>f</sup>	77.78 <sup>b</sup>	67.88 <sup>g</sup>	69.90 <sup>e</sup>	74.61 <sup>c</sup>	0.1986	0.0001
FDRGM	$C_{ab}^*$	16.99 <sup>e</sup>	23.14 <sup>c</sup>	23.32 <sup>c</sup>	25.85 <sup>a</sup>	25.70 <sup>a</sup>	24.71 <sup>b</sup>	22.38 <sup>d</sup>	24.72 <sup>b</sup>	24.54 <sup>b</sup>	0.2150	0.0001
FDSM	$L^*$	75.61 <sup>g</sup>	79.41 <sup>f</sup>	79.69 <sup>ef</sup>	80.63 <sup>de</sup>	81.98 <sup>c</sup>	87.67 <sup>a</sup>	75.69 <sup>g</sup>	80.61 <sup>cd</sup>	83.50 <sup>b</sup>	0.2710	0.0001
FDSM	$a^*$	12.61 <sup>a</sup>	10.98 <sup>c</sup>	8.70 <sup>f</sup>	11.84 <sup>b</sup>	10.33 <sup>d</sup>	9.41 <sup>e</sup>	11.35 <sup>bc</sup>	8.31 <sup>f</sup>	8.39 <sup>f</sup>	0.0817	0.0001
FDSM	$b^*$	18.73 <sup>f</sup>	26.44 <sup>c</sup>	28.06 <sup>d</sup>	23.68 <sup>de</sup>	27.65 <sup>b</sup>	31.43 <sup>a</sup>	23.37 <sup>e</sup>	24.41 <sup>d</sup>	27.41 <sup>b</sup>	0.1835	0.0001
FDSM	$h_{ab}^*$	66.08 <sup>f</sup>	67.48 <sup>e</sup>	72.82 <sup>b</sup>	63.47 <sup>f</sup>	69.55 <sup>d</sup>	73.37 <sup>a</sup>	64.13 <sup>f</sup>	71.23 <sup>c</sup>	73.02 <sup>a</sup>	0.2610	0.0001
FDSM	$C_{ab}^*$	22.58 <sup>e</sup>	28.63 <sup>b</sup>	29.38 <sup>a</sup>	26.48 <sup>c</sup>	29.52 <sup>a</sup>	29.81 <sup>a</sup>	25.98 <sup>d</sup>	25.79 <sup>d</sup>	28.67 <sup>b</sup>	0.1915	0.0001
FDRSM	$L^*$	74.27 <sup>d</sup>	76.04 <sup>c</sup>	76.51 <sup>c</sup>	78.80 <sup>b</sup>	78.71 <sup>b</sup>	80.49 <sup>a</sup>	73.45 <sup>e</sup>	78.84 <sup>b</sup>	80.48 <sup>a</sup>	0.1310	0.0001
FDRSM	$a^*$	6.62 <sup>c</sup>	5.69 <sup>d</sup>	5.61 <sup>d</sup>	9.29 <sup>a</sup>	9.58 <sup>a</sup>	8.45 <sup>b</sup>	9.62 <sup>a</sup>	7.92 <sup>b</sup>	6.36 <sup>c</sup>	0.0882	0.0001
FDRSM	$b^*$	22.53 <sup>b</sup>	22.51 <sup>b</sup>	22.49 <sup>b</sup>	22.87 <sup>b</sup>	22.65 <sup>b</sup>	23.79 <sup>a</sup>	21.78 <sup>c</sup>	22.61 <sup>b</sup>	24.09 <sup>a</sup>	0.1091	0.0001
FDRSM	$h_{ab}^*$	75.91 <sup>b</sup>	75.85 <sup>b</sup>	76.03 <sup>a</sup>	67.93 <sup>d</sup>	67.11 <sup>d</sup>	70.48 <sup>c</sup>	66.20 <sup>e</sup>	70.73 <sup>c</sup>	75.25 <sup>b</sup>	0.2645	0.0001
FDRSM	$C_{ab}^*$	14.53 <sup>d</sup>	23.22 <sup>c</sup>	23.18 <sup>c</sup>	24.69 <sup>b</sup>	24.59 <sup>b</sup>	25.25 <sup>a</sup>	25.66 <sup>a</sup>	23.98 <sup>c</sup>	24.92 <sup>b</sup>	0.0152	0.0001

Small letters in the same row indicate that means are significantly different ( $P < 0.0001$ ) related to temperature and time (Tukey's test). GM, *Gluteus Medius*; SM, *Semimembranosus*; FD, freeze dried; R, rehydrated; RSME, root mean square error;  $L^*$ , lightness;  $a^*$ , red to green;  $b^*$ , yellow to blue; A, 24 h drying cycle; B, 48 h drying cycle; C, 72 h drying cycle.

$R^2 = 0.998$  [-50 °C];  $R^2 = 0.951$  [-60 °C]); FDRSM ( $R^2 = 0.986$  [-40 °C];  $R^2 = 0.993$  [-50 °C];  $R^2 = 0.969$  [-60 °C]) (Fig. 2). WAC values decreased when freezing temperature decreased. Lower WAC values were obtained at -60 °C in both muscles. Decrease in WAC is due to smaller ice crystals formed at -60 °C, leading to smaller pore sizes, which in turn gave considerably higher values of surface area which decreases rehydration in samples.

In general, results obtained showed that in bovine muscles colour parameters and physicochemical parameters reflected higher changes when freeze drying was applied at -50 and -60 °C than -40 °C, as it was stated above this can be due to that a higher number of smaller pore sizes in solids, which led to a higher surface area to oxygen exposure and a thinner size of muscle fibre possibly enhanced oxygen penetration through solids, increasing changes in the samples.

#### Texture analysis

Significant differences between values ( $P < 0.0001$ ) were obtained for texture parameters (Table 2). Positive values were obtained for ASM, ENT, CON, COR and HOM. In texture analysis, COR indicates the linearity of the image. For an image with large areas of similar intensities, a high value of correlation is measured. HOM shows the level of uniformity on the

image. High values of HOM showed improvement of uniformity and smoothness of the images (Karimi *et al.*, 2012). ENT is a measure of randomness, and takes low values for smooth images. ASM represents the smoothness of an image, when ASM is high the image has very similar pixels. CON is a measure that shows the difference from one pixel to others close to it. It is a measure of local grey variations. Low values in CON represent diminish of local variation of pixels. The softer the texture, the lower the contrast, which is due to lower pixel value difference between two neighbours. On the other hand, increases in softness are due to reduction in hardness, which can be attributed to its porous structure.

CFDRSM and CFDRGM showed higher COR, HOM and ASM; and lower values of ENT and CON when they were compared to CFDSM and CFDGM. In CFDRSM and CFDRGM, lower values of COR were obtained at higher freezing temperature (-40 °C); Higher ASM values were obtained at higher freezing temperature (-40 °C); Higher ENT values at lower freezing temperature (-60 °C); Higher HOM values at higher freezing temperature (-40 °C) and lower CON values at higher freezing temperature (-40 °C). Significant differences were also observed for drying time. Image texture analysis revealed that when freezing process is carried out at higher freezing



**Table 2** Texture analysis of *Semimembranosus* and *Gluteus Medius* muscles (Sp: Aberdeen Angus)

Sample	Parameter	-40 °C			-50 °C			-60 °C			RSME	P value
		A	B	C	A	B	C	A	B	C		
CFDGM	COR	0.86 <sup>f</sup>	0.99 <sup>a</sup>	0.84 <sup>g</sup>	0.90 <sup>b</sup>	0.87 <sup>e</sup>	0.89 <sup>c</sup>	0.88 <sup>d</sup>	0.88 <sup>d</sup>	0.86 <sup>d</sup>	0.0238	0.0001
CFDGM	ASM	0.26 <sup>g</sup>	0.23 <sup>h</sup>	0.29 <sup>e</sup>	0.27 <sup>f</sup>	0.31 <sup>d</sup>	0.22 <sup>h</sup>	0.43 <sup>c</sup>	0.48 <sup>b</sup>	0.54 <sup>a</sup>	0.0158	0.0001
CFDGM	ENT	6.53 <sup>d</sup>	6.80 <sup>ab</sup>	6.38 <sup>e</sup>	6.70 <sup>c</sup>	6.58 <sup>d</sup>	6.85 <sup>a</sup>	5.96 <sup>e</sup>	5.94 <sup>e</sup>	5.96 <sup>e</sup>	0.0893	0.0001
CFDGM	HOM	0.90 <sup>cd</sup>	0.92 <sup>bc</sup>	0.91 <sup>d</sup>	0.92 <sup>b</sup>	0.92 <sup>b</sup>	0.90 <sup>cd</sup>	0.96 <sup>a</sup>	0.96 <sup>a</sup>	0.95 <sup>a</sup>	0.0077	0.0001
CFDGM	CON	0.18 <sup>c</sup>	0.21 <sup>a</sup>	0.20 <sup>b</sup>	0.15 <sup>e</sup>	0.17 <sup>d</sup>	0.18 <sup>c</sup>	0.07 <sup>g</sup>	0.07 <sup>g</sup>	0.10 <sup>f</sup>	0.0044	0.0001
CFDRGM	COR	0.88 <sup>b</sup>	0.86 <sup>c</sup>	0.90 <sup>a</sup>	0.86 <sup>c</sup>	0.86 <sup>c</sup>	0.85 <sup>d</sup>	0.85 <sup>d</sup>	0.86 <sup>c</sup>	0.85 <sup>d</sup>	0.0275	0.0001
CFDRGM	ASM	0.57 <sup>c</sup>	0.70 <sup>a</sup>	0.68 <sup>ab</sup>	0.68 <sup>ab</sup>	0.64 <sup>d</sup>	0.64 <sup>d</sup>	0.40 <sup>e</sup>	0.44 <sup>d</sup>	0.44 <sup>d</sup>	0.0254	0.0001
CFDRGM	ENT	5.36 <sup>e</sup>	5.35 <sup>e</sup>	5.36 <sup>e</sup>	5.49 <sup>bc</sup>	5.51 <sup>b</sup>	5.52 <sup>b</sup>	5.67 <sup>a</sup>	5.51 <sup>b</sup>	5.52 <sup>b</sup>	0.1204	0.0001
CFDRGM	HOM	0.98 <sup>a</sup>	0.95 <sup>d</sup>	0.97 <sup>b</sup>	0.97 <sup>b</sup>	0.97 <sup>b</sup>	0.97 <sup>b</sup>	0.96 <sup>c</sup>	0.97 <sup>b</sup>	0.96 <sup>c</sup>	0.0063	0.0001
CFDRGM	CON	0.04 <sup>e</sup>	0.04 <sup>e</sup>	0.05 <sup>d</sup>	0.05 <sup>d</sup>	0.06 <sup>c</sup>	0.06 <sup>c</sup>	0.09 <sup>a</sup>	0.09 <sup>a</sup>	0.07 <sup>b</sup>	0.0031	0.0001
CFDSM	COR	0.90 <sup>d</sup>	0.94 <sup>a</sup>	0.94 <sup>a</sup>	0.90 <sup>d</sup>	0.88 <sup>f</sup>	0.93 <sup>b</sup>	0.89 <sup>e</sup>	0.92 <sup>c</sup>	0.88 <sup>f</sup>	0.0270	0.0001
CFDSM	ASM	0.38 <sup>b</sup>	0.29 <sup>d</sup>	0.33 <sup>c</sup>	0.40 <sup>b</sup>	0.43 <sup>a</sup>	0.35 <sup>c</sup>	0.40 <sup>b</sup>	0.35 <sup>c</sup>	0.29 <sup>d</sup>	0.0148	0.0001
CFDSM	ENT	6.41 <sup>bc</sup>	6.76 <sup>a</sup>	6.31 <sup>cd</sup>	6.40 <sup>bc</sup>	6.42 <sup>bc</sup>	6.41 <sup>bc</sup>	5.72 <sup>e</sup>	6.23 <sup>d</sup>	6.52 <sup>b</sup>	0.0990	0.0001
CFDSM	HOM	0.09 <sup>c</sup>	0.10 <sup>bc</sup>	0.10 <sup>bc</sup>	0.10 <sup>bc</sup>	0.11 <sup>b</sup>	0.10 <sup>bc</sup>	0.10 <sup>bc</sup>	0.08 <sup>c</sup>	0.12 <sup>a</sup>	0.0044	0.0001
CFDSM	CON	0.95 <sup>a</sup>	0.95 <sup>a</sup>	0.95 <sup>a</sup>	0.95 <sup>a</sup>	0.95 <sup>a</sup>	0.96 <sup>a</sup>	0.96 <sup>a</sup>	0.96 <sup>a</sup>	0.93 <sup>b</sup>	0.0077	0.0001
CFDRSM	COR	0.88 <sup>a</sup>	0.88 <sup>a</sup>	0.86 <sup>b</sup>	0.86 <sup>b</sup>	0.84 <sup>c</sup>	0.86 <sup>b</sup>	0.82 <sup>d</sup>	0.82 <sup>d</sup>	0.81 <sup>c</sup>	0.0246	0.0001
CFDRSM	ASM	0.70 <sup>c</sup>	0.73 <sup>b</sup>	0.75 <sup>a</sup>	0.57 <sup>f</sup>	0.57 <sup>f</sup>	0.56 <sup>f</sup>	0.60 <sup>e</sup>	0.64 <sup>d</sup>	0.61 <sup>e</sup>	0.0151	0.0001
CFDRSM	ENT	5.45 <sup>d</sup>	5.40 <sup>e</sup>	5.39 <sup>e</sup>	5.26 <sup>f</sup>	5.40 <sup>e</sup>	5.52 <sup>b</sup>	5.49 <sup>c</sup>	5.66 <sup>a</sup>	5.51 <sup>b</sup>	0.0379	0.0001
CFDRSM	HOM	0.97 <sup>bc</sup>	0.97 <sup>bc</sup>	0.99 <sup>a</sup>	0.98 <sup>b</sup>	0.97 <sup>bc</sup>	0.98 <sup>b</sup>	0.97 <sup>bc</sup>	0.97 <sup>bc</sup>	0.96 <sup>c</sup>	0.0031	0.0001
CFDRSM	CON	0.04 <sup>c</sup>	0.04 <sup>c</sup>	0.04 <sup>c</sup>	0.04 <sup>c</sup>	0.05 <sup>b</sup>	0.05 <sup>b</sup>	0.05 <sup>b</sup>	0.06 <sup>a</sup>	0.06 <sup>a</sup>	0.0044	0.0001

Small letters in the same row indicate that means are significantly different ( $P < 0.0001$ ) related to freeze drying cycle (Tukey's test). GM, *Gluteus Medius*; SM, *Semimembranosus*; FD, Freeze dried; R, Rehydrated; A, 40 °C/24 h; B, 40 °C/48 h; C, 40 °C/72 h; RSME, root mean square error. COR, correlation; ASM, energy; ENT, entropy; HOM, homogeneity; CON, contrast.

temperature (-40 °C) in both bovine muscles, uniformity, smoothness, softness and linearity of the image reveal better texture profile when compared to lower freezing temperature. On the other hand, SEM images of CFDSM and CFDGM revealed that freeze-dried bovine muscles had higher pore size and lower account of pores at higher freezing temperature (-40 °C) and a homogeneous structure at higher drying time (72 h). Temperatures at -50 and -60 °C showed smaller pore size and higher amount of pores related to formation of ice crystals. Higher amounts of pores with smaller pore size decreases rehydration process due to a higher inner surface. Image analysis revealed that texture is affected by pore size and amount, so rehydration process is also affected. Samples are harder, smoothness uniformity and linearity of the image obtained decrease.

## Conclusions

Colour, texture and physicochemical properties were evaluated in different freeze drying cycles in two bovine muscles to be applied in instant meal. Results revealed that analysed parameters were less affected when freeze drying cycle was performed at higher freezing temperatures (-40 °C) and higher drying time (72 h). Freeze drying cycle is very important because

smaller pore sizes increase surface area and decrease rehydration process, texture, colour and other quality attributes can be affected. In the future, other quality parameters must be evaluated to complete the study.

## References

- Baker, G., Sims, C., Gorbet, D., Sanders, T. & O'keefe, S. (2002). Storage water activity effect on oxidation and sensory properties of high-oleic peanuts. *Journal of Food Science*, **67**, 1600–1603.
- Bald (1991). Ice crystal growth in idealised freezing system. In: *Food Freezing: Today and Tomorrow* (edited by W.B. Bald). Pp. 67–80. London/New York: Springer-Verlag.
- Bevilacqua, A. & Zaritzky, N. (1980). Ice morphology in frozen beef. *International Journal of Food Science & Technology*, **15**, 589–597.
- Faustman, C., Sun, Q., Mancini, R. & Suman, S. (2010). Myoglobin and lipid oxidation interactions: mechanistic bases and control. *Meat Science*, **86**, 86–94.
- Girolami, A., Napolitano, F., Faraone, D. & Braghieri, A. (2013). Measurement of meat colour using a computer vision system. *Meat Science*, **93**, 111–118.
- Harnkarnsujarit, N., Kawai, K. & Suzuki, T. (2014). Effects of freezing temperature and water activity on microstructure, color, and protein conformation of freeze-dried bluefin tuna (*Thunnus orientalis*). *Food Bioprocess Technology*, **8**, 916–925.
- Jeong, J., Kim, G., Yang, H. & Joo, S. (2011). Effect of freeze-thaw cycles on physicochemical properties and color stability of beef *Semimembranosus* muscle. *Food Research International*, **44**, 3222–3228.
- Karimi, M., Fathi, M., Sheykholeslam, Z., Sahraiyani, B. & Naghipoor, F. (2012). Effect of different processing parameters on

- quality factors and image texture features of bread. *Journal of Bioprocess and Biotechnology*, **2**, 12–17.
- Kiani, H. & Sun, D. (2011). Water crystallisation and its importance to freezing of foods: a review. *Trends in Food Science and Technology*, **22**, 407–426.
- Koc, B., Eren, I. & Kaymak, F. (2008). Modelling bulk density, porosity and shrinkage of quince during drying: the effect of drying method. *Journal of Food Engineering*, **85**, 340–349.
- Kong, F., Tang, J., Lin, M. & Rasco, B. (2008). Thermal effects on chicken and salmon muscles: tenderness, cook loss, area shrinkage collagen solubility and microstructure. *LWT-Food Science and Technology*, **41**, 1210–1222.
- Kono, S., Kawamura, I., Yamagami, S., Araki, T. & Sagara, Y. (2014). Optimum storage temperature of frozen cooked rice predicted by ice crystal measurement, sensory evaluation and artificial neural network. *International Journal of Refrigeration*, **56**, 165–172.
- Leelayuthsoontorn, P. & Thipayarat, A. (2006). Textural and morphological changes of Jasmine rice under various elevated cooking conditions. *Food Chemistry*, **96**, 606–613.
- Maltini, E., Torreggiani, D., Venir, E. & Bertolo, G. (2003). Water activity and the preservation of plant food. *Food Chemistry*, **82**, 79–88.
- Mendoza, F., Lu, R., Diwan, A., Cen, H. & Bailey, B. (2012). Integrated spectral and image analysis of hyperspectral scattering data for prediction of apple fruit firmness and soluble solids content. *Postharvest Biology and Technology*, **62**, 149–160.
- Messina, V., Sancho, A., Grigioni, G. et al. (2014). Evaluation of different bovine muscles to be applied in freeze drying for instant meal. Study of physicochemical and senescence parameters. *Animal*, **9**, 723–772.
- Mounir, S. (2015). Texturing of chicken breast meat as an innovative way to intensify drying: use of a coupled washing/diffusion CWD phenomenological model to enhance kinetics and functional properties. *Drying Technology*, **33**, 1369–1381.
- Muhamad, I. & Karim, N. (2014). Trends, Convenience, and Safety Issues of Ready Meals. Food Engineering Series, 2014 Editor: Springer, 105–123.
- Oikonomopoulou, V., Krokida, M. & Karathanos, V. (2011a). Structural properties of freeze-dried rice. *Journal of Food Engineering*, **107**, 326–333.
- Oikonomopoulou, V., Krokida, M. & Karathanos, V. (2011b). The influence of freeze drying conditions on microstructural changes of food products. *Procedia Food Science*, **1**, 647–654.
- Reyes, A., Perez, N. & Mahn, A. (2011). Theoretical and experimental study of freeze –drying “loco” (*Concholepas concholepas*). *Drying Technology*, **29**, 1386–1395.
- Saini, M., Singh, J. & Prakash, N. (2014). Analysis of wheat grain varieties using image processing – a review. *International Journal of Scientific Research*, **3**, 490–495.
- Vasiliki, P., Magdalini, K. & Vaios, T. (2011). The influence of freeze drying conditions on microstructural changes of food products. *Procedia Food Science*, **1**, 647–654.

### Supporting Information

Additional Supporting Information may be found in the online version of this article:

**Figure S1.** Scanning micrographs performed at 500 time’s magnification of cross sectional of cooked freeze dried (CFD) and cooked freeze dried rehydrated (CFDR) Gluteus medius muscle (GM) at different freeze drying cycles.